Necessity of Conserved Asparagine Residues in the Leucine-Rich Repeats of Platelet Glycoprotein Ibα for the Proper Conformation and Function of the Ligand-Binding Region†

Vahid Afshar-Kharghan,‡ Garunee Gineys,‡ Alicia J. Schade,§ Lily Sun,‡ Chester Q. Li,‡ Larry V. McIntire,§ Jing-Fei Dong,‡ and José A. López*,‡,||

Division of Hematology/Oncology, Department of Internal Medicine, and Department of Molecular and Human Genetics, Baylor College of Medicine and Veterans Affairs Medical Center, Houston, Texas 77030, and Cox Laboratory for Bioengineering, Rice University, Houston, Texas 77251

Received September 2, 1999; Revised Manuscript Received December 14, 1999

ABSTRACT: The polypeptides of the platelet von Willebrand factor (vWf) receptor, the GP Ib-IX-V complex, each contain tandem repeats of a sequence that assigns them to the leucine-rich repeat protein family. Here, we studied the role of conserved Asn residues in the leucine-rich repeats of GP Ibα, the ligand-binding subunit of the complex. We replaced the Asn residue in the sixth position of the first or sixth leucine-rich repeat (of seven) either with a bulky, charged Lys residue or with a Ser residue (sometimes found in the same position of other leucine-rich repeats) and studied the effect of the mutations on complex expression, modulator-dependent vWf binding, and interactions with immobilized vWf under fluid shear stress. As predicted, the Lys substitutions yielded more severe phenotypes, producing proteins that either were rapidly degraded within the cell (mutant N158K) or failed to bind vWf in the presence of ristocetin or roll on immobilized vWf under fluid shear stress (mutant N41K). The binding of function-blocking GP Ibα antibodies to the N41K mutant was either significantly reduced (AK2 and SZ2) or abolished (AN51 and CLB-MB45). Ser mutations were tolerated much better, although both mutants demonstrated subtle defects in vWf binding. These results suggest a vital role for the conserved asparagine residues in the leucine-rich repeats of GP Ibα for the structure and functions of this polypeptide. The finding that mutations in the first leucine-rich repeat had a much more profound effect on vWf binding indicates that the more N-terminal repeats may be directly involved in this interaction.

Assignment of proteins to the large and diverse leucine-rich repeat family is based on their possession of a conserved motif containing one or several tandem copies of a 22−28 amino acid sequence with a characteristic spacing of leucine residues (*1*−*3*). Members of this family are phylogenetically widespread and are not united by common functions or cellular locations. They are found in the cell nucleus, in the cytoplasm, in internal granules, and on the plasma membrane, or can be secreted to become plasma proteins or constituents of the extracellular matrix. They subserve such distinct functions as DNA repair, signal transduction, cell adhesion, and hormone binding (*1*, *2*, *4*). On human platelets, all of the known members of this family belong to a large plasma membrane complex known as the glycoprotein (GP)[1] Ib-IX-V complex (*5*). This complex plays vital roles in the hemostatic functions of the platelets, following vessel injury by adhering the platelets to the vessel wall through an interaction with von Willebrand factor (vWf), and by providing a high-affinity binding site on the plasma membrane for thrombin through which low concentrations of this potent platelet agonist can activate platelets (*6*). Recently, this complex was also shown to constitute a platelet receptor for P-selectin, through which the platelets can interact with activated endothelium (*7*).

The GP Ib-IX-V complex comprises four polypeptide subunits, GP Ibα, GP Ibβ, GP IX, and GP V, which are present on the platelet plasma membrane in a stoichiometry of 2:2:2:1, respectively (*1*). Each is oriented as a type I transmembrane protein, and each also contains a leucine-rich motif in its extracellular N-terminus, with GP Ibα containing seven tandem leucine-rich repeats (*8*, *9*), GP Ibβ (*10*) and GP IX (*11*) each containing one copy, and GP V containing fifteen tandem repeats (*12*, *13*).

Aside from the conserved spacing of leucines, the consensus sequences for the repeats in almost all leucine-rich

† This work was supported by NIH Grants HL02463, HL46416, HL18673, and NS23327, the Robert A. Welch Foundation Grant C938, a Grant-in-Aid from the American Heart Association,Texas Affiliate, and the NIH Medical Scientist Training Program at the Baylor College of Medicine.

* To whom correspondence should be addressed at Hematology/Oncology (111H), Veterans Affairs Medical Center, 2002 Holcombe Blvd., Houston, TX 77030. Phone: (713) 794-7088. Fax: (713) 794-7578. E-mail: josel@bcm.tmc.edu.

‡ Division of Hematology/Oncology, Department of Internal Medicine, Baylor College of Medicine and Veterans Affairs Medical Center.

§ Rice University.

|| Department of Molecular and Human Genetics, Baylor College of Medicine and Veterans Affairs Medical Center.

[1] Abbreviations: α-MEM, α-minimal essential medium; BSA, bovine serum albumin; FBS, fetal bovine serum; FITC, fluorescein isothiocyanate; PBS, phosphate-buffered saline; GP, glycoprotein; vWf, von Willebrand factor; mRNA, messenger RNA.

10.1021/bi992061j CCC: $19.00
Published on Web 03/02/2000

repeat proteins contain asparagine in the sixth position. Of the GP Ib-IX-V polypeptides, only four of the twenty-four repeats do not contain Asn in this position. The residues that replace Asn all contain small, hydrophilic side chains (Ser, Thr, or Cys), which are likely to maintain the structure of the region. In a leucine-rich repeat protein for which the three-dimensional structure has been determined, porcine ribonuclease inhibitor, either Asn or Cys in this position appears to be crucial for allowing a transition from a β strand to a $\beta\alpha$ loop (*14*).

Because the GP Ibα ligand-binding domain (His1−Glu282) also contains the seven tandem leucine-rich repeats, we sought to define how mutations of conserved asparagines within the repeats would influence GP Ibα expression and ligand-binding properties. We mutated the Asn in the first and sixth leucine-rich repeats, replacing it either with a bulky charged residue, Lys, or with a residue that is tolerated in other leucine-rich repeats, Ser. Here, we describe the results of these changes on the conformation, synthesis, and vWf-binding function of the GP Ib-IX-V complex.

MATERIALS AND METHODS

Glycoprotein Ibα Mutagenesis, Cell Lines, and Transfections. Mutagenesis of the GP Ibα cDNA was carried out by the method of Deng and Nickloff (*15*), with primers that incorporated changes of one or two nucleotides to alter the relevant codons. The mutations were carried out directly in the GP Ibα expression plasmid, pDX-GP Ibα. Mutant plasmids were sequenced completely to verify that only the intended mutations were made. To construct cell lines expressing the full GP Ib-IX complex (GP Ibα, GP Ibβ, and GP IX are the minimal requirements for efficient cell-surface expression of a functional complex), the mutant GP Ibα plasmids were transfected into CHO βIX cells, which have stable, high-level expression of GP Ibβ and GP IX (*16*). Also cotransfected was the plasmid pREP4, which carries a hygromycin-resistance gene that allows for drug selection of the transfectants. The transfections were carried out by liposome-mediated DNA delivery as described (*17*). Expression of cell-surface GP Ibα in drug-resistant cells was assayed by flow cytometry after the cells were labeled with the GP Ibα monoclonal antibody WM23 (kindly provided by Dr. Michael C. Berndt, Baker Medical Research Institute, Melbourne, Australia). This antibody is directed against an epitope in the mucin-like macroglycopeptide region of GP Ibα, and is unlikely to be affected by the mutations, which affect a different domain of the protein. Cell lines were periodically sorted for higher expression by selection of the high-expressing cells with antibody-coupled magnetic beads. For this, cells were detached with 0.53 mM EDTA and resuspended in phosphate-buffered saline (PBS) containing 1% bovine serum albumin (BSA). The cells were incubated first with WM23 for 30 min at room temperature and then with magnetic beads coated with sheep anti-mouse IgG (Dynabeads, Dynal, Inc., Lake Success, NY). Bead-bound cells were separated from unbound cells on a magnetic apparatus (Dynal).

The studies to examine the effect of the mutations on the cell-surface expression of the GP Ib-IX complex relied only on transient transfection of the wild-type and mutant cDNAs. Briefly, CHO βIX cells were transfected with a cDNA encoding either wild-type GP Ibα or one of the Asn mutants, and the cells were examined by flow cytometry 72 h after the transfection after the cells were labeled with WM23.

Flow Cytometry. Flow cytometric assessment of GP Ibα surface expression was essentially performed as previously described (*18*). Cells detached with 0.53 mM EDTA were incubated with WM23 (1 μg/mL) for 30 min at room temperature. After the cells were washed with PBS to remove unbound antibody, they were incubated with fluorescein isothiocyanate (FITC)-conjugated rabbit anti-mouse IgG (Zymed, South San Francisco, CA) in the dark for 30 min at room temperature. The cells were then analyzed on a FACScan flow cytometer (Becton Dickinson, San Jose, CA), stimulating with laser light at 488 nm and collecting light emitted at >520 nm. The same procedure was used to evaluate the expression of epitopes for the GP Ibα monoclonal antibodies AK2, AN51, SZ2, and CLB-MB45, all of which bind within the N-terminal 282 amino acids of GP Ibα.

Metabolic Labeling and Immunoprecipitation of Normal and Mutant GP Ibα Polypeptides. Cells expressing wild-type and mutant GP Ib-IX complexes were grown in 100 mm cell-culture dishes. For radiolabeling, the cells were first washed in cysteine-free α-minimal essential medium (α-MEM; Life Technologies, Inc., Grand Island, NY) and then incubated in this medium for 30 min before addition of 100 μCi of [^{35}S]cysteine (ICN, Irvine, CA). The cells were incubated in the radioactive medium for 4 h, the medium was then removed, and the cells were washed several times in PBS. The cells were then lysed in lysis buffer (100 mM Tris, pH 7.4, 10 μg/mL leupeptin, 1.6 μg/mL benzamidine, 0.1 mg/mL soybean trypsin inhibitor, 1 mM phenylmethylsulfonyl fluoride, and 1% digitonin) and centrifuged at 10000*g* for 5 min to remove debris. The lysate was then incubated with formaldehyde-fixed *Staphylococcus aureus* cells (Pansorbin beads, Calbiochem, San Diego, CA) to remove nonspecifically bound proteins (4 h, 4 °C). The beads were removed by centrifugation, WM23 (10 μg/mL) was added and incubated for 4 h, and Pansorbin beads that had been preequilibrated with rabbit anti-mouse IgG (5 μg/mL, 4 h) were then added to the lysate. After a 4 h incubation, the beads were collected by centrifugation at 10000*g* for 5 min, resuspended, and washed twice in cell lysis buffer. The beads were then boiled for 5 min in SDS sample buffer to remove the bound proteins, which were then loaded onto reducing SDS−polyacrylamide gels (7.5% acrylamide). After electrophoresis, the gels were dried on a gel dryer and evaluated by autoradiography on a Fuji Phosphorimager (model BAS 1000).

Immunolabeling of Cells and Fluorescence Microscopy. Cells grown to confluence on glass chamber slides (Titertek, Nunc, Naperville, IL) were washed with PBS, fixed with 4% paraformaldehyde (Sigma Chemical, St. Louis, MO), and permeabilized in 0.1% Triton X-100 (Sigma). The cells were then incubated with WM23 (5 μg/mL) for 1 h, washed several times with PBS, incubated with FITC-conjugated goat anti-mouse IgG for 1 h, and washed again several times with PBS. The slides were then sealed and stored in the dark at 4 °C until they were examined. Microscopy was performed on an Olympus IX50 microscope, and photographed onto Fuji Neopan 1600 black-and-white film.

RT-PCR. We evaluated transcription from the cells transfected with the various mutant GP Ibα plasmids, by reverse

transcription/polymerase chain reaction (RT-PCR) of cellular RNA. Total RNA was extracted from 10^6-10^7 transfected cells using a commercial kit (RNeasy Mini kit, QIAGEN, Valencia, CA), and 3−5 μg of RNA was used for each RT-PCR reaction. Each reverse transcription reaction contained the following: RNA (3−5 μg), reverse primer (GGTCTTCAGCTCATTGCCTT, 0.75 μM), 5 mM $MgCl_2$, 1 mM dNTP, 1 U/μL RNase inhibitor, 2 μL of 10% PCR buffer (500 mM KCl, 100 mM Tris−HCl), and MuLV reverse transcriptase (2.5 U/μL). The reaction was brought to 20 μL with diethyl pyrocarbonate-treated distilled water. The mixture was incubated at 42 °C for 15 min, and the resultant reverse transcription product was then denatured by heating at 99 °C for 5 min. The following were then added to the tube: forward primer (CTGTGAGGTCTCCAAAGTGG, final concentration 0.75 μM), 8 μL of the manufacturer's PCR buffer, 2.5 units of *AmpliTaq* DNA polymerase, and 4 μL of 25 mM $MgCl_2$. The total volume of each reaction tube was bought to 100 μL with distilled water. The reverse transcription product was then amplified by PCR by first heating the sample to 95 °C for 2 min and then subjecting it to 35 cycles of 95 °C for 45 s, 60 °C for 60 s, and 72 °C for 90 s. The RT-PCR products were analyzed by 2% agarose gel electrophoresis. MuLV reverse transcriptase, *AmpliTaq* DNA polymerase, PCR buffer, and RNase inhibitor were all purchased from Perkin-Elmer (Foster City, CA).

vWf Binding by Flow Cytometry. Cells expressing wild-type or mutant GP Ib-IX complexes were detached from culture plates with 0.53 mM EDTA, washed, and suspended at 1×10^6 cells/mL in 1 mL of PBS containing 1% BSA to block nonspecific binding (10 min, room temperature). A 5 μg sample of vWf (provided by Dr. Michael Berndt) and 1.5 mg of ristocetin (Sigma, St. Louis, MI) were added to each tube and incubated at room temperature. After 30 min the cells were vigorously dispersed and washed with PBS. They were then incubated with rabbit anti-vWf antibody (Dako, Carpinteria, CA) at 1 μg/mL for 1 h at room temperature. The cells were then washed twice in PBS and incubated with FITC-conjugated goat anti-rabbit antibody (Zymed) for another 30 min. The cells were washed twice more with PBS, and their surface fluorescence was analyzed by flow cytometry.

To correct for the effect on vWf binding of variations in surface expression of GP Ibα between cell lines, an aliquot of the cells analyzed for vWf binding was analyzed simultaneously for GP Ibα surface expression by flow cytometry after labeling with WM23, and the binding values were corrected for the relative differences in surface expression. The binding to CHO αβIX cells was arbitrarily designated as 100%, and the binding values from the other cell lines were normalized on the basis of their relative surface levels.

Iodination of vWf and Assay of Ligand Binding. Purified human vWf was iodinated with Na[^{125}I] by the Iodogen method as described (*19*) and purified on a Sephadex G25 column (Pharmacia Laboratories, Piscataway, NJ). The binding of the radiolabeled ligand was assessed as previously described (*19*). Briefly, cells expressing wild-type or mutant GP Ibα were detached with EDTA and resuspended in Tyrode's buffer to a final concentration of 4×10^7 cells/mL. A 25 μL sample of the cell suspension was placed into each of 10 Eppendorf tubes. ^{125}I-labeled vWf was added to duplicate sets of five tubes at final concentrations of 0, 0.3, 0.6, 1.2, 2.4, and 4.8 μg/mL. Ristocetin was then added to both sets of tubes to a final concentration of 1.4 mg/mL. The final reaction volume was adjusted to 100 μL with Tyrode's buffer. The mixture was incubated at room temperature for 30 min and then layered onto a column containing 30% sucrose. Membrane-bound vWf was separated from free vWf by centrifugation at 10000*g* for 5 min. The capillary tips of the column containing the cell pellets were cut off, and the radioactivity was counted in a γ counter. The binding specificity was determined by incubating CHO βIX cells with ^{125}I-labeled vWf and ristocetin. All direct binding data were normalized to correct for differences in surface levels of the complex.

Cell Rolling on Immobilized vWf. The experiments to examine the interaction between cells expressing wild-type or mutant GP Ib-IX complexes and immobilized vWf under flow were carried out in a parallel-plate flow chamber consisting of a polycarbonate block, a silicon gasket, and a glass coverslip coated with vWf. Experiments using such a flow chamber system have been described previously (*20*). Briefly, purified human vWf was coated onto glass coverslips by incubating the coverslips with a vWf solution (50 μg/mL) for 45 min at room temperature. Before each experiment, a coated coverslip was washed with PBS and assembled in the parallel-plate flow chamber such that the coverslip formed the bottom of the chamber. The three components of the chamber were held together by a vacuum. A syringe pump connected to the outlet port draws fluid through the chamber at defined flow rates to generate desired shear stresses (*21*). The flow chamber was mounted onto an inverted-stage microscope (DIAPHOT-TMD; Nikon, Garden City, NY) equipped with a silicon-intensified target video camera (model C2400; Hammatus, Waltman, MA) connected to a video cassette recorder. To induce cell rolling on immobilized vWf, a cell suspension (100 000 cells/mL) was perfused through the chamber at flow rates calculated to generate fluid shear stresses of 5, 10, and 15 dyn/cm^2. Cell rolling in a single-view field was recorded in real time for 3 min, and the video data were then analyzed off-line using imaging software (IC-300 Modular Image Processing Workstation, Inovision Corp., Durham, NC) to calculate the rolling velocities of 50 or more cells per run. Each experiment was performed at least three times independently. Cells considered to be rolling were those observed to be moving in the direction of fluid flow while maintaining constant contact with the vWf matrix. Both the number of rolling cells and their rolling velocity were calculated (*22*, *23*). The distance a single cell rolled during a defined period determined the rolling velocity; the mean velocity was calculated by averaging the velocities of all the rolling cells in each experiment.

Statistical Analysis. Statistical analysis used in this study included the Student's *t* test and linear regression analysis. Statistically significant differences were defined as those in which the p value was <0.05.

RESULTS

Mutation of Conserved Asparagine Residues in the Leucine-Rich Repeats of GP Ibα. One important structural feature of the repeats in virtually all proteins of the leucine-

A.

GP Ibα	L	X	L	S	X	N	X	L	T	T	L	P	X	G	L	L	X	X	L	P	X	L	S	X
GP Ibβ	L	V	L	T	G	N	N	L	T	A	L	P	P	G	L	L	D	A	L	P	A	L	R	T
GP IX	L	L	L	A	N	N	S	L	Q	S	V	P	P	G	A	F	D	H	L	P	Q	L	Q	T
GP V	L	X	L	X	X	N	X	L	X	X	L	P	X	X	X	F	X	X	L	X	X	L	X	X
Consensus	L	X	L	X	X	N	X	L	X	X	L	P	X	G	L	L	X	X	L	P	X	L	X	X

B.

LRR1	36	L	H	L	S	E	N	L	L	Y	T	F	S	L	A	T	L	M	P	Y	T	R	L	T	Q	59
LRR2	60	L	N	L	D	R	C	E	L	T	K	L	Q	V	D	G	T	L	P	V	L	G	T	-	-	81
LRR3	82	L	D	L	S	H	N	Q	L	Q	S	L	P	L	L	G	Q	T	L	P	A	L	T	V	-	104
LRR4	105	L	D	V	S	F	N	R	L	T	S	L	P	L	G	A	L	R	G	L	G	E	L	Q	E	128
LRR5	129	L	Y	L	K	G	N	E	L	K	T	L	P	P	G	L	L	T	P	T	P	K	L	E	K	152
LRR6	153	L	S	L	A	N	N	N	L	T	E	L	P	A	G	L	L	N	G	L	E	N	L	D	T	176
LRR7	177	L	L	L	Q	E	N	S	L	Y	T	I	P	K	G	F	F	G	S	H	L	L	P	F	A	200

Mutations:

(LRR1) Asn41
→Lys
→Ser

(LRR6) Asn158
→Lys
→Ser

FIGURE 1: (A) Consensus sequences of the leucine-rich repeats of the polypeptides of the GP Ib-IX-V complex. The consensus sequences of the seven GP Ibα and fifteen GP V leucine-rich repeats are shown, along with the sequences of the lone GP Ibβ and GP IX leucine-rich motifs. (B) Leucine-rich repeats of GP Ibα. The Asn residues mutated in the current studies are highlighted.

rich repeat family is the presence of asparagine in the sixth position of the consensus sequence, implying an important role for this residue in the structures of leucine-rich motifs (*3*). The consensus sequences of the leucine-rich repeats of the polypeptides of the GP Ib-IX-V complex are shown in Figure 1A, with the asparagine residues highlighted. Figure 1B depicts the sequence of the seven leucine-rich repeats of GP Ibα with the mutated Asn residues highlighted. We chose to mutate the Asn residues in leucine-rich repeats 1 and 6 because these repeats are toward opposite ends of the leucine-rich motif and because repeat 1 is not bounded on the N-terminus by another repeat while repeat 6 is bounded on both sides by other leucine-rich repeats. Thus, mutations to the two repeats may have different effects on adjacent repeat sequences. The Asn in these sequences was replaced by either Lys or Ser. (The mutants are designated N41S, N41K, N158S, and N158K.) The Lys substitution is predicted to cause a more profound change in the structure, as the side chain adds both bulk and charge. The Ser substitution was chosen because this amino acid has a less bulky side chain, is sometimes found at this position in other leucine-rich repeat proteins, and differs from Cys—the only amino acid other than Asn found in this position of leucine-rich repeat consensus sequences—only in having an oxygen atom instead of a sulfur. Cys was not chosen because of its potential for forming disulfide bonds.

Effect of Mutation of Conserved Asparagine Residues on GP Ib-IX Complex Expression. We studied the biosynthetic consequences of the mutations by both transient and stable transfection. Transient transfection studies revealed that all of the mutants but N158K were expressed on the cell surface (Figure 2). Both of the N41 mutations decreased expression of the mutant GP Ibα in comparison to the wild-type polypeptide (Figure 2). With respect to expression of the N158K mutant, we found the same results in stable cell lines selected by growth in hygromycin-containing medium, with none of the resistant clones from the N158K transfection expressing GP Ibα on the cell surface. These data suggested one of three possibilities for the fate of the N158K mutant: (1) that the mutation had such a severe effect on the structure of the polypeptide that it was degraded shortly after its synthesis, (2) that the mutant was sequestered within an intracellular compartment and failed to be secreted, or (3) that the mutation destabilized the mRNA encoding the protein and precluded its translation. We were able to rule out the second possibility by microscopy of permeabilized, fluorescently labeled cells. The N158S, N41K, and N41S mutants all showed staining patterns with fluorescently labeled antibody similar to that of the cells expressing wild-type GP Ibα, with most of the polypeptide appearing on the cell surface (Figure 3). In contrast, cells transfected with the N158K mutant had no detectable protein, either on the plasma membrane or within the cell (Figure 3, panel E).

To further investigate the fate of the mutants, we metabolically labeled the cells with [^{35}S]cysteine and immunoprecipitated the labeled GP Ibα with WM23. The results reflected the microscopy studies. Again, all of the mutants were precipitated from their respective cell lines, except N158K, for which not even a faint band was detected (Figure 4A).

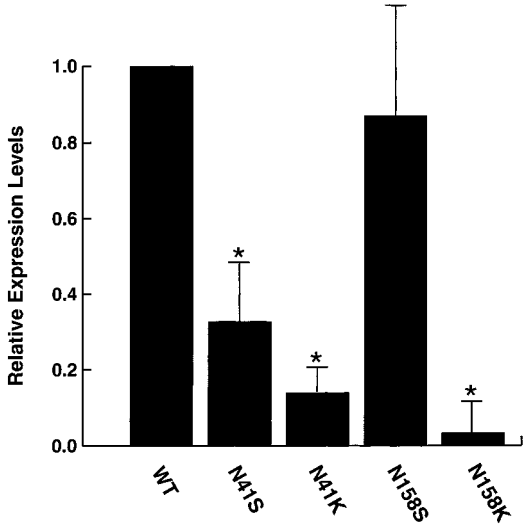

FIGURE 2: Effects of the Asn mutations of GP Ibα on the cell surface expression of the GP Ib-IX complex. The Asn mutants were transiently transfected into CHO βIX cells, and the expression of the mutants was determined by flow cytometry after the cells were surface labeled with the monoclonal GP Ibα antibody WM23. The values depicted are the relative fluorescence values calculated from the mean fluorescence values for each mutant averaged from seven separate transient transfection studies, after the background fluorescence of sham-transfected cells was subtracted. The value for the wild-type GP Ibα transfections is arbitrarily designated as 1.0. All mutants except N158K were expressed on the cell surface. The asterisk indicates $p < 0.001$ for comparison with wild-type GP Ibα (Student's t test, $n = 7$).

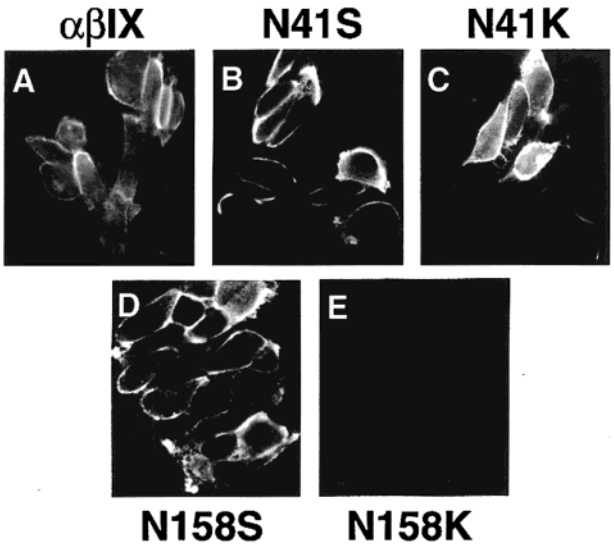

FIGURE 3: Immunofluorescence microscopy of GP Ibα mutant-expressing cell lines. Cells stably expressing wild-type GP Ibα or the Asn mutants were fixed and permeabilized with 0.1% Triton X-100, and GP Ibα was then labeled with fluorescent WM23. The GP Ibα distribution in all of the cell lines was similar, except in the N158K mutant, in which no GP Ibα could be identified.

To determine whether mRNA instability caused by the mutation was the cause of the failure to express the mutant, mRNA was purified from the CHO αβIX, CHO βIX, and N158K lines and reverse transcribed, and a GP Ibα-specific fragment was amplified using the polymerase-chain reaction. This experiment showed that the cells expressing N158K contained similar amounts of GP Ibα mRNA as did the cells expressing wild-type GP Ibα (Figure 4B), indicating that the

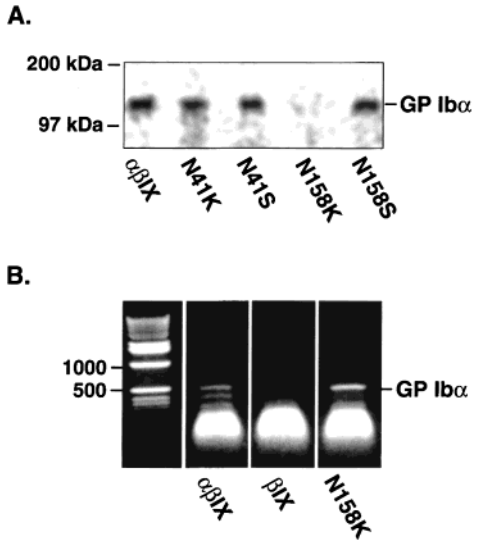

FIGURE 4: (A) The N158K mutation yields an unstable polypeptide. GP Ibα from ^{35}S-metabolically-labeled cells was immunoprecipitated with WM23. Only the N158K polypeptide was undetectable. (B) RT-PCR of mRNA from cell lines expressing wild-type GP Ibα and the N158K mutant. RNA was reverse transcribed and the cDNA fragment amplified by PCR. Cells expressing wild-type GP Ibα or the N158K mutant produced the expected band, whereas CHO βIX (which lacks GP Ibα) did not.

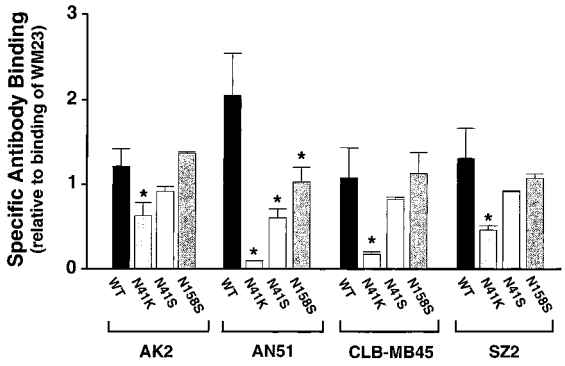

FIGURE 5: Antibody binding to the Asn mutants. The binding of GP Ibα antibodies to the mutant polypeptides as measured by flow cytometry and expressed as the binding relative to the binding of WM23, which binds C-terminal to the GP Ibα ligand-binding region. The N41K mutation affected the binding of all of the antibodies, most severely affecting the binding of AN51 and CLB-MB45. All of the antibodies listed bind within the first 282 amino acids of GP Ibα.

failure of the mutant to be expressed on the cell surface resulted from its rapid posttranslational degradation.

Antibody Binding to the Mutants. We next examined the binding to the cells of four monoclonal antibodies against GP Ibα with epitopes in the N-terminus to determine whether any of them could detect a mutation-induced conformational change. Their binding was compared to the binding of WM23 (Figure 5). As expected, none of the antibodies bound the N158K cells (data not shown). Of the other mutants, N41K was the most severely affected. The binding of two of the antibodies, AN51 and MB45, was eliminated by the mutation. One of these, AN51, has been shown to inhibit ristocetin-induced platelet aggregation, possibly by binding directly to a vWf-binding site (*24*). This antibody also bound at lower levels to the cells expressing either the N41S mutant or the N158S mutant.

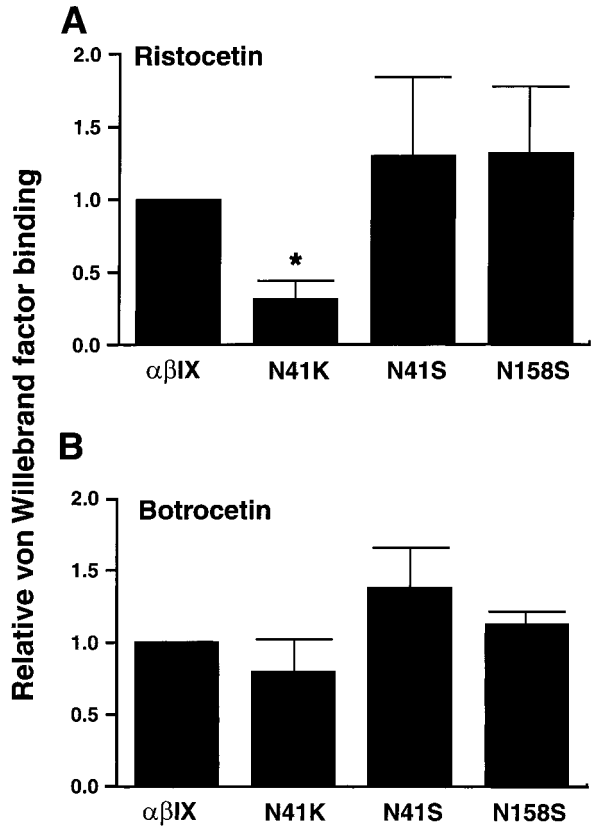

FIGURE 6: Ristocetin- and botrocetin-induced vWf binding to the GP Ibα mutants measured by flow cytometry using a fluorescently labeled rabbit anti-vWf antibody. Binding is expressed relative to the binding to CHO α*β*IX cells, which was arbitrarily set as 100%. (A) Ristocetin-induced vWf binding decreased significantly in the N41K mutants (Student's *t* test, $n = 6$, $p < 0.01$), whereas the binding to cells expressing the Ser mutants was similar to the binding to cells expressing wild-type GP Ibα ($n = 6$, $p = 0.34$). (B) Botrocetin-induced vWf binding was not affected by any of the mutations.

von Willebrand Factor Binding. We examined the ability of the mutant cell lines to support ristocetin- and botrocetin-induced vWf binding. This was done in two ways. First, we examined binding by a flow cytometric assay. After the cells were incubated with vWf at concentrations saturating for wild-type GP Ibα and the appropriate modulator, they were washed, and bound vWf was detected with a rabbit anti-vWf polyclonal antibody, followed by FITC-labeled goat anti-rabbit IgG. Cell fluorescence was then evaluated by flow cytometry. This technique has the advantage over more conventional binding techniques in that it allows analysis of binding on a cell-by-cell basis. When vWf binding was induced by ristocetin, only the N41K mutant demonstrated a defect in binding, with the binding being at background levels (Figure 6A). In contrast, botrocetin-induced binding did not distinguish any of the mutants from wild-type GP Ibα (Figure 6B).

The dose-response binding of vWf induced by ristocetin was also studied using iodinated vWf. The N41K mutant was again found to be completely defective in binding. In addition, this method revealed diminished binding to the N41S mutant (Figure 7).

Adhesion to and Rolling on Immobilized vWf of Cells Expressing the GP Ibα Mutants. We have recently shown that cells expressing GP Ib-IX or GP Ib-IX-V complexes

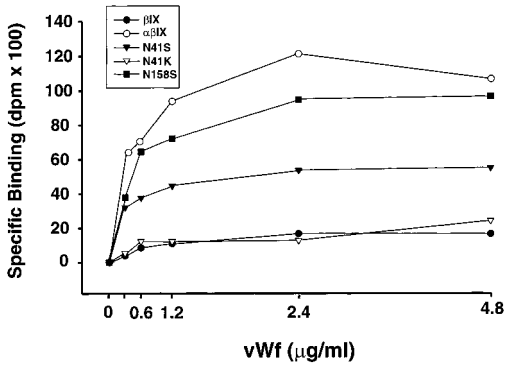

FIGURE 7: Ristocetin-induced binding of ^{125}I-labeled vWf. Cells expressing wild-type or mutant GP Ibα were incubated with increasing concentrations of ^{125}I-labeled vWf. At the three highest concentrations of vWf, vWf binding was significantly lower to the N41 mutants than to wild-type vWf (Student's *t* test, $n = 3$, $p < 0.001$).

can adhere to and roll on immobilized vWf in a process analogous to the adhesion of platelets to subendothelial vWf in the vessel wall (*20*). This adhesion occurs in the absence of modulators and thus represents a more physiological test of vWf binding. We therefore examined the adhesion of cells expressing wild-type and mutant GP Ib-IX complexes to vWf immobilized on glass coverslips. The cells were perfused over the immobilized vWf at shear stresses of 5, 10, and 15 dyn/cm^2 in a parallel-plate flow chamber (*20*). We evaluated two functional parameters: cell attachment and cell rolling velocity. The N41K mutant again demonstrated the most severe functional defect: cells expressing this mutant neither attached nor rolled on the immobilized vWf. On the other hand, cells expressing N41S and N158S both attached to the vWf matrix, albeit less efficiently than cells expressing wild-type GP Ibα. Of the two Ser mutants, the defect in N41S was more severe, with significantly fewer cells attaching at 5 and 10 dyn/cm^2 and no cells attaching at 15 dyn/cm^2 (Figure 8B). In addition, those cells that did attach rolled faster than both the wild-type cells and the N158S cells, indicating a more rapid off-rate to the interaction (Figure 8A).

DISCUSSION

The studies reported here confirm a vital role for conserved asparagine residues in the leucine-rich repeats of GP Ibα for the structure and functions of this polypeptide. We chose to mutate this residue because it is conserved in the repeats of the four GP Ib-IX-V polypeptides, all of which belong to the leucine-rich repeat superfamily of proteins. Kajava (*4*) has proposed that this superfamily can be divided into six subfamilies, on the basis of the length and consensus sequence of the leucine-rich repeats. Even with this subdivision of the family, all but one of the groups have Asn in this position; in the remaining subgroup it is replaced by Cys. In porcine ribonuclease inhibitor, the Asn or Cys residue determines the site at which a β strand ends, giving way to a $\beta-\alpha$ loop that precedes an α helix (*14*). A similar structure has been predicted for the leucine-rich repeats of other members of this superfamily (*25*).

The repeating motifs yield an orderly structure with the α helices stacking on the outer face and the β strands stacking on the inner face to form a parallel β sheet. With the

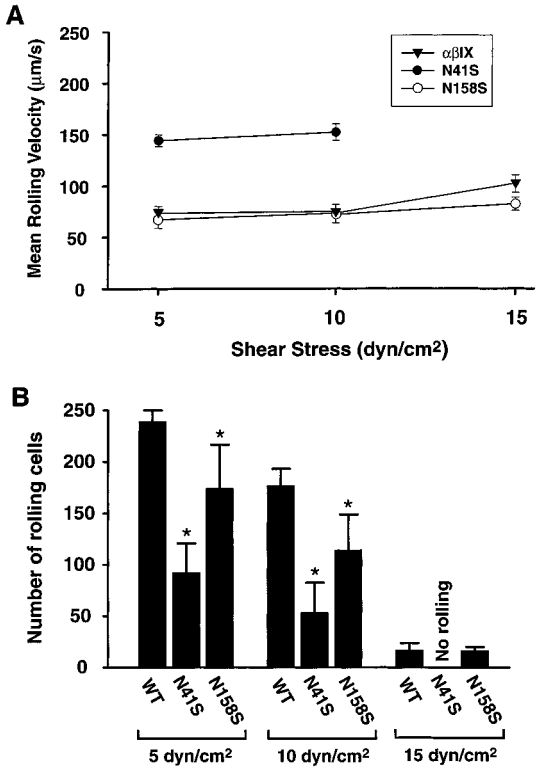

FIGURE 8: Rolling of cells expressing the Asn mutants on immobilized vWf under fluid shear stress. Interactions between the Asn mutants and immobilized vWf were studied under fluid shear stress using a parallel-plate flow chamber system. Cells expressing either the wild-type or the mutant complexes were perfused over glass coverslips coated with vWf under fluid shear stresses ranging from 5 to 15 dyn/cm^2. The number of cells that rolled along the matrix and their rolling velocity under different shear stresses were then calculated. Cells expressing the N41K mutant failed to roll on immobilized vWf under any of the shear stresses tested. (A) Cells expressing the N41S mutant rolled faster than the other two cell lines at 5 and 10 dyn/cm^2 (Student's t test, $n = 145-576$, $p < 0.001$) and failed to attach at 15 dyn/cm^2. (B) The number of rolling cells for all the cell types decreased with increasing shear stress, but the decrease was greater for the cells expressing the Ser mutants than for cells expressing wild-type GP Ibα (Student's t test, $n = 4$, $p < 0.05$).

exception of the first and last repeats in a series, the β strands are stabilized by hydrogen bonding with the neighboring two strands of the sheet (*14*). The side chains of the conserved Asn residues also stabilize the structure, being buried and forming hydrogen bonds with the polypeptide backbone. The 15 leucine-rich repeats of porcine ribonuclease inhibitor form a semicircular structure, with the helices facing outward and the β sheet forming the inner surface (*14*). This arrangement allows for the formation of a large inner surface comprising the solvent-exposed β sheet through which the protein interacts with ribonuclease A (*26*). Mutations that prevent the orderly stacking of the repeats would be expected to preclude formation of this surface and thus to prevent ligand binding.

Such a structural disruption of GP Ibα by the Asn mutations provides a feasible explanation for our results. As predicted, replacement of Asn with Lys disrupted the structure most severely, yielding a protein that was rapidly degraded when the residue in leucine-rich repeat 6 was mutated (mutant N158K), and producing a protein that did not bind function-blocking monoclonal antibodies (AN51 and CLB-MB45) or vWf in the presence of ristocetin when the first repeat was mutated (N41K). The N158K mutant was degraded so rapidly that we were unable to detect it by any of several techniques (Figures 2, 3, and 4A), yet the cells transfected with the mutant plasmid contained similar amounts of mRNA as did cells expressing wild-type GP Ibα (Figure 4B). The N41K mutant, although expressed on the cell surface, was severely defective in terms of its ability to bind vWf, whether induced by ristocetin or under flow in a parallel-plate flow chamber. In the latter assay, cells expressing N41K neither attached to nor rolled on the immobilized vWf.

The profound effect of the N41K mutation and the subtler defect of the N41S mutation on vWf binding are consistent with our recent studies with canine−human GP Ibα chimeras (*27*). Here, both ristocetin-induced vWf binding and adhesion to vWf under flow were eliminated in cell lines expressing the GP Ib-IX complex when the human GP Ibα sequence was replaced with the corresponding canine sequence to the end of the second leucine-rich repeat. Ristocetin-induced vWf binding was recovered when the chimera containing the entire N-terminus to residue 282 was "rehumanized" to the end of the fourth leucine-rich repeat, an indication that the most N-terminal sequences of GP Ibα play a vital role in vWf binding. Also of interest was that these chimeras enabled the mapping of epitopes for function-blocking GP Ibα antibodies. Most of those that inhibited ristocetin-induced vWf binding and adhesion of GP Ib-IX complex-expressing cells to vWf under flow mapped to the N-terminus, from residue 1 to residue 59, including AN51, whose epitope was abolished by the N41K mutation.

Obviously, the N158K mutation had a much more severe effect on the structure of the polypeptide than did the N41K mutation. This might be accounted for by the location of the mutations. If, as proposed, the mutations affect the orderly stacking of the leucine-rich repeats, N158K, because it affects an internal repeat, would disrupt the relationship of repeat 6 with both repeat 5 and repeat 7. On the other hand, N41K affects the relationship of repeat 1 with only one other repeat, repeat 2, which may explain why this mutation is tolerated better than the N158K mutation.

The Ser mutations had a much milder effect on structure. Both mutant polypeptides reached the cell surface at levels comparable to that of wild-type GP Ibα, but they still did not function completely normally in terms of vWf binding. The ristocetin-induced binding properties of cells expressing N158S were indistinguishable from those of cells expressing wild-type GP Ibα, but the mutation did have a subtle defect detectable in the parallel-plate flow chamber, where fewer of the N158S cells attached to the vWf matrix than did wild-type cells. The defect in the N41S mutant was more severe, being manifested both in the ristocetin-induced binding assay and in the parallel-plate flow chamber. Ristocetin-induced vWf binding of N41S-expressing cells was half that of cells expressing wild-type GP Ibα, and the cells rolled twice as fast in the flow chamber at equivalent shear stresses and failed to attach at shear stresses above 10 dyn/cm^2. Thus, mutation in the first repeat more severely affected vWf binding, which suggests that the more N-terminal repeats are directly involved in the interaction with vWf, consistent with data derived from our studies of canine−human GP Ibα chimeras (*27*). An effect on the epitope for AN51, an antibody that blocks the interaction with vWf, also points to a direct involvement of this region in vWf binding.

In summary, the findings reported here demonstrate that the structure of the GP Ibα leucine-rich repeats is vital for the synthesis and vWf-binding functions of the GP Ib-IX-V complex.

REFERENCES

1. López, J. A. (1994) *Blood Coagul. Fibrinolysis 5*, 97−119.
2. Kobe, B., and Deisenhofer, J. (1995) *Curr. Opin. Struct. Biol. 5*, 409−416.
3. Kobe, B., and Deisenhofer, J. (1994) *Trends Biochem. Sci. 19*, 415−421.
4. Kajava, A. V. (1998) *J. Mol. Biol. 277*, 519−527.
5. López, J. A., and Dong, J. F. (1997) *Curr. Opin. Hematol. 4*, 323−329.
6. Jamieson, G. A. (1997) *Thromb. Haemostasis 78*, 242−246.
7. Romo, G. M., Dong, J. F., Schade, A. J., Gardiner, E. E., Li, C., Kansas, G. S., McIntire, L. V., Berndt, M. C., and López, J. A. (1999) *J. Exp. Med. 190*, 803−813.
8. Lopez, J. A., Chung, D. W., Fujikawa, K., Hagen, F. S., Papayannopoulou, T., and Roth, G. J. (1987) *Proc. Natl. Acad. Sci. U.S.A. 84*, 5615−5619.
9. Titani, K., Takio, K., Handa, M., and Ruggeri, Z. M. (1987) *Proc. Natl. Acad. Sci. U.S.A. 84*, 5610−5614.
10. Lopez, J. A., Chung, D. W., Fujikawa, K., Hagen, F. S., Davie, E. W., and Roth, G. J. (1988) *Proc. Natl. Acad. Sci. U.S.A. 85*, 2135−2139.
11. Hickey, M. J., Deaven, L. L., and Roth, G. J. (1990) *FEBS Lett. 274*, 189−192.
12. Hickey, M. J., Hagen, F. S., Yagi, M., and Roth, G. J. (1993) *Proc. Natl. Acad. Sci. U.S.A. 90*, 8327−8331.
13. Lanza, F., Morales, M., de La Salle, C., Cazenave, J.-P., Clemetson, K. J., Shimomura, T., and Phillips, D. R. (1993) *J. Biol. Chem. 268*, 20801−20807.
14. Kobe, B., and Deisenhofer, J. (1993) *Nature 366*, 751−756.
15. Deng, W. P., and Nickoloff, J. A. (1992) *Anal. Biochem. 200*, 81−88.
16. López, J. A., Weisman, S., Sanan, D. A., Sih, T., Chambers, M., and Li, C. Q. (1994) *J. Biol. Chem. 269*, 23716−23721.
17. Li, C. Q., Dong, J.-F., Lanza, F., Sanan, D. A., Sae-Tung, G., and López, J. A. (1995) *J Biol. Chem. 270*, 16302−16307.
18. Dong, J.-F., Li, C. Q., Sae-Tung, G., Hyun, W., Afshar-Kharghan, V., and López, J. A. (1997) *Biochemistry 36*, 12421−12427.
19. Dong, J.-F., Li, C. Q., and López, J. A. (1994) *Biochemistry 33*, 13946−13953.
20. Fredrickson, B. J., Dong, J. F., McIntire, L. V., and López, J. A. (1998) *Blood 92*, 3684−3693.
21. Slack, S. M., and Turitto, V. T. (1994) *Thromb. Haemostasis 72*, 777−781.
22. Jones, D. A., Abbassi, O., McIntire, L. V., McEver, R. P., and Smith, C. W. (1993) *Biophys. J. 65*, 1560−1569.
23. Kukreti, S., Konstantopoulos, K., Smith, C. W., and McIntire, L. V. (1997) *Blood 89*, 4104−4111.
24. Ruan, C., Tobelem, G., McMichael, A. J., Drouet, L., Legrand, Y., Degos, L., Kieffer, N., Lee, H., and Caen, J. P. (1981) *Br. J. Haematol. 49*, 511−519.
25. Kajava, A. V., Vassart, G., and Wodak, S. J. (1995) *Structure. 3*, 867−877.
26. Kobe, B., and Deisenhofer, J. (1995) *Nature 374*, 183−186.
27. Shen, Y., Romo, G. M., Dong, J. F., Schade, A. J., McIntire, L. V., Kenny, D., Whisstock, J. C., Berndt, M. C., López, J. A., and Andrews, R. K. (2000) *Blood 95*, 903−910.

BI992061J